Water Resources Research

RESEARCH ARTICLE
10.1029/2019WR026098

Two Improvements to Gardner's Method of Measuring the Hydraulic Conductivity of Non-saturated Media: Accounting for Impedance Effects and Non-constant Imposed Suction Increment

Filip Stanić[1,2], Pierre Delage[1], Yu-Jun Cui[1], Emmanuel De Laure[1], Pierre-Antoine Versini[2], Daniel Schertzer[2], and Ioulia Tchiguirinskaia[2]

[1]Ecole des Ponts ParisTech, Navier/CERMES, Marne la Vallée, France, [2]Ecole des Ponts ParisTech, HM&Co, Marne la Vallée, France

Key Points:
- Gardner developed the first analytical method for determining the hydraulic conductivity function based on transient outflow data
- Kunze and Kirkham developed a graphical method to account for impedance effects, that is nowadays replaced by numerical back analysis
- The new proposed analytical method appears to be more reliable than Kunze and Kirkahm's method and simpler than numerical back analysis

Supporting Information:
- Supporting Information S1

Correspondence to:
F. Stanić,
filip.stanic@enpc.fr

Citation:
Stanić, F., Delage, P., Cui, Y.-J., De Laure, E., Versini, P.-A., Schertzer, D., & Tchiguirinskaia, I. (2020). Two improvements to Gardner's method of measuring the hydraulic conductivity of nonsaturated media: Accounting for impedance effects and nonconstant imposed suction increment. *Water Resources Research*, *56*, e2019WR026098. https://doi.org/10.1029/2019WR026098

Received 7 AUG 2019
Accepted 30 NOV 2019
Accepted article online 28 DEC 2019

Abstract Gardner's (1956, https://doi.org/10.2136/sssaj1956.03615995002000030006x) transient method of measuring the hydraulic conductivity function of unsaturated media has been largely used, together with the improved graphical method proposed by Kunze and Kirkham (1962, https://doi.org/10.2136/sssaj1962.03615995002600050006x) to account for the impedance effect resulting from using a low hydraulic conductivity ceramic disk in porous plate testing. These methods are nowadays seldom used, since they have been replaced by numerical back analysis and methods for parameter optimization. Based on tests carried out on a specific device allowing to determine the water retention and transport properties of water in a coarse granular media at low suctions (up to 50 kPa), it was found necessary to account (i) for impedance effects and (ii) for the effects of nonconstant suction increments, as is often the case when using the hanging column technique. A new method is proposed to account for impedance effects, based on an analytical solution of the equations governing water transfer. The validity of this method is tested by considering experimental data from three distinct materials: a coarse green roof volcanic substrate, poorly graded sand, and undisturbed silty clay. Compared to the graphical method Kunze and Kirkham's method, it is less operator-dependent and hence more objective. It is also simpler than numerical back analysis methods, since it does not require any use of numerical code or parameter optimization algorithm, providing a more direct and reliable access to the hydraulic conductivity. An analytical solution is also proposed to solve the problem resulting from the application of a nonconstant suction increment.

1. Introduction

Gardner's method (Gardner, 1956) was the first analytical method of calculating the hydraulic conductivity of unsaturated porous media by measuring, in the pressure plate apparatus, the transient outflow resulting from a step increase in suction, applied to the unsaturated specimen through an increase in air pressure. This method is based on various assumptions, including the linearity of the water retention curve (WRC) and a constant value of the diffusivity D over the suction increment applied (both hypotheses are better fulfilled with small suction increments). Gardner's method does not account for the impedance effects of the plate (made up of a saturated ceramic porous disk with high air entry value) that may have a significantly lower hydraulic conductivity than that of the saturated specimen. This impedance effect was considered for first time by Miller and Elrick (1958), who proposed an analytical method to account for the flow resistance exerted by the disk, provided the disk hydraulic conductivity was known and the contact specimen/disk was perfect. Rijtema (1959) improved the method by developing a solution based on the hydraulic conductivity ratio between the soil and the disk, valid regardless of the quality of the specimen/disk contact. Finally, Kunze and Kirkham (1962) developed a graphical method based on Miller and Elrick's method, in which particular attention was focused on the accurate determination of initial outflow values, which is particularly important with respect to impedance effects. However, this method, based on fitting experimental data against normalized charts to obtain some specific parameters required to calculate the hydraulic conductivity, may present some degree of subjectivity and operator dependency (see Appendix B). More recently, Valiantzas (1990) proposed an analytical method that was not based on the assumption of constant diffusivity. The method was applied on single-step outflow measurements (Doering, 1965) by using an iterative algorithm to determine the relationship between the diffusivity and the water content. The main disadvantage of

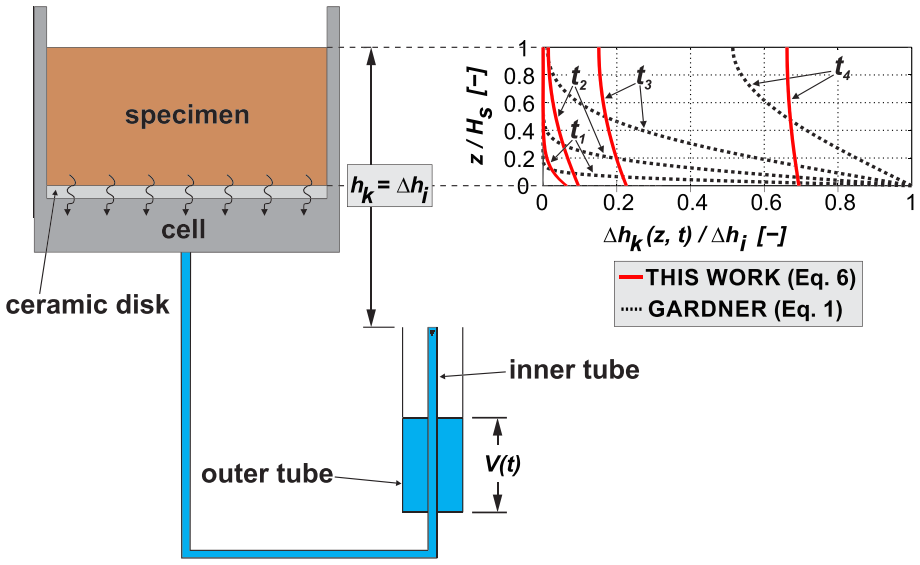

Figure 1. Simplified scheme of the hanging column apparatus of Stanić et al. (2019), where the water drained from the specimen overflows from the inner to the outer tube (initial suction equal to 0).

this method is that the WRC, necessary to make the calculations, has to be determined independently of the hydraulic conductivity function (HCF).

In the past decades, numerical back analysis methods have been preferred to determine the HCF of unsaturated soils, through the simulation of water flow in unsaturated media by numerically solving Richards equation (Richards, 1931). When dealing with techniques in which ceramic stones are involved, numerical back analysis methods account for impedance effects by simulating transient water outflows from two-layered specimens (soil specimen and ceramic disk) subjected to suction increments (Durner & Iden, 2011; Eching et al., 1994; Eching & Hopmans, 1993; Nasta et al., 2011; Schelle et al., 2011; van Dam et al., 1994; Wayllace & Lu, 2011). In these calculations, different functions are used to describe the hydraulic properties of the soils. Their parameter values are obtained by using different optimization algorithms for minimizing the deviation between measured and simulated outflows (Levenberg, 1944; Šimunek et al., 2008). Since the WRC of the investigated materials cannot be always reliably interpreted with these functions that depend either on one (Brooks & Corey, 1964) or several semiempirical parameters (van Genuchten, 1980; Fredlund & Xing, 1994; etc.), the HCF derived through Mualem's (1976) approach does not necessarily provide realistic results (e.g., Khaleel & Relyea, 1995).

Given the advantages and drawbacks of existing methods, a new and simple analytical approach to account for impedance effects in the determination of the HCF of unsaturated soils is proposed in this paper, together with an approach to account for nonconstant imposed suction increment. The validation of the method is carried out based on experimental data from three different materials, that is, a coarse material used as substrate in an urban green roof located in the Paris area and called the “Green Wave” because of its wavy shape (Stanić et al., 2019; Versini et al., 2018), a poorly graded sand and an undisturbed silty clay (Wayllace & Lu, 2011). This analytical method is simpler than numerical back analysis methods since it does not require the use of any numerical code and sophisticated optimization tools. It is also not affected either by any subjective graphical method like in the traditional Kunze and Kirkham's method.

2. Methods

2.1. Analytical Methods of Determining the Hydraulic Conductivity of Unsaturated Materials

The methods developed in this work originate from an experimental investigation carried out by Stanić et al. (2019). The experimental device used for the determination of the HCF based on Gardner's and Kunze and Kirkham's methods is presented in a simplified way in Figure 1 and 2 (see Stanić et al., 2019, for more details). It consists of a metal cylindrical cell in which specimen is placed on a high air entry value ceramic porous disk. In Figure 1, one observes that a suction step can be applied through a hanging column device,

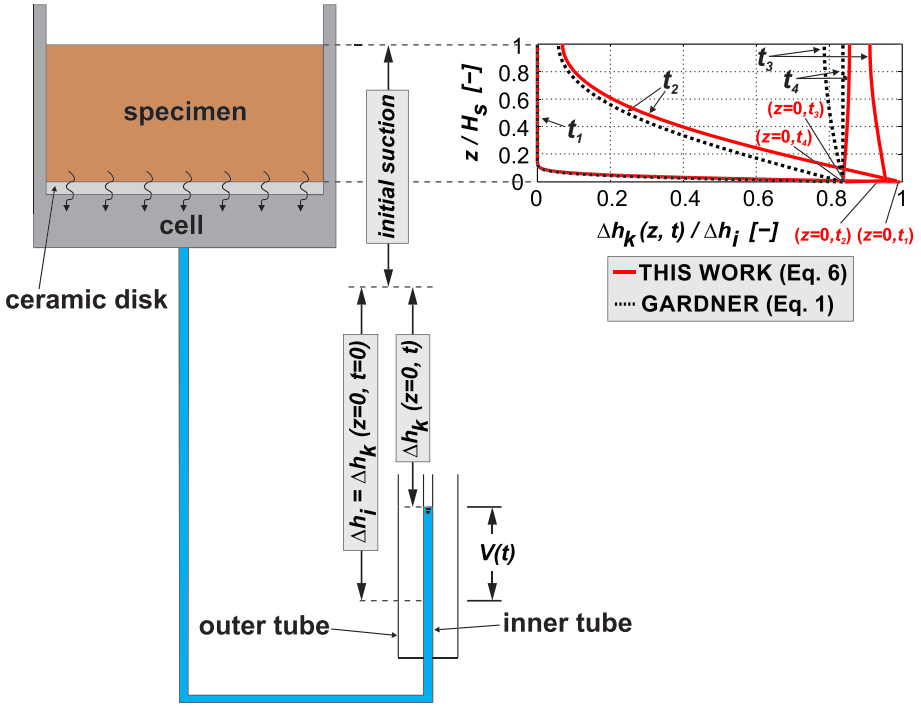

Figure 2. Simplified scheme of Stanic et al.'s (2019) device, in the case when the water extracted from the specimen is collected in the inner tube (no overflow), resulting in a nonconstant suction step.

by moving down a mobile system in which the constant suction is controlled by the level of the top of the inner thin tube. The water extracted due to the suction step overflows in the outer tube and is determined by monitoring the change in water height by means of a high precision differential pressure gauge (Stanić et al., 2019).

In hanging column systems, it is convenient to express suction in water height $h_k(z, t)$, as the sum of the initially established hydrostatic suction profile $h_k(z, t{=}0)$ and the time depending change of suction $\Delta h_k(z, t)$. The imposed suction increment Δh_i (L) (index i for "imposed") impacts the gradient $\frac{\partial h_k(z,t)}{\partial z}\Big|_{z=0}$ that induces the outflow at the specimen bottom (see Appendix A).

If the hydraulic conductivity of the ceramic disk is higher than that of the specimen (no impedance effects), the constant Δh_i is immediately transferred to the specimen bottom ($\Delta h_k(z{=}0, t) = \Delta h_i = const.$) — see dotted lines in Figure 1. In this case, the assumptions made by Gardner's method (linearity of the WRC along the small suction step applied and constant diffusivity over the same Δh_i) allow to express $\Delta h_k(z, t)$ using Fourier's series, based on the analogy with Terzaghi-Fröhlich consolidation equation (Terzaghi & Fröhlich, 1936) that governs the consolidation of saturated soils:

$$\Delta h_k(z,t) = \Delta h_i\left(1-\frac{4}{\pi}\sum_{n=1,3,5\ldots}^{\infty}\frac{1}{n}e^{-(n/2)^2\pi^2\frac{tD(h_k)}{H_s^2}}\sin\frac{n}{2}\frac{\pi z}{H_s}\right) \quad (1)$$

where $D(h_k) = K(h_k)/C(h_k)$ is the (constant) diffusivity value (L^2/T) at suction h_k, where $K(h_k)$ (L/T) is the hydraulic conductivity and $C(h_k)$ (L^{-1}) the slope of the WRC along the applied suction step. Suction h_k is a reference value equal to the sum of the initial suction and Δh_i. Equation (1) concerns the outflow (see Appendix A), which is integrated in time to obtain the changes in water volume:

$$V(t) = V_\infty\left(1-\frac{8}{\pi^2}\sum_{n=1,3,5\ldots}^{\infty}\frac{1}{n^2}e^{-(n\pi/2)^2\ \mathrm{t}\ \mathrm{D}(h_k)/H_s^2}\right) \quad (2)$$

where V_∞ is the total volume (L^3) of the outflow drained from the soil specimen after imposing Δh_i.

Without considering the outflow at very small t, Gardner provided a convenient relation by keeping only the first term of Fourier series:

$$ln(V_\infty - V(t)) = ln\left(\frac{8V_\infty}{\pi^2}\right) - \left(\frac{\pi}{2H_s}\right)^2 D(h_k)t \tag{3}$$

Indeed, Gardner showed that the changes in the first term with respect to time become linear after a short time period (see Stanić et al., 2019), providing a reliable estimation of the diffusivity $D(h_k)$ from the slope of the $ln(V_\infty - V(t))$ curve. The estimation is more accurate with small imposed suction increments, since $D(h_k)$ is the average diffusivity value along it. The hydraulic conductivity at suction h_k is derived as $K(h_k) = D(h_k)C(h_k)$.

When the hydraulic conductivity of the disk is significantly smaller than that of the specimen, the suction increment Δh_i imposed at the bottom of the porous disk is not immediately transferred to the specimen due to impedance effects. To cope with this issue, Kunze and Kirkham (1962) proposed a graphical method that is described in more details in Appendix B. As commented in section 1, this graphical method is nowadays rarely used and has been replaced by numerical back analysis of water outflow under imposed suction increments.

2.2. A New Method to Account for Impedance Effects

As an alternative to existing methods of accounting for impedance effects, it is proposed to first apply Darcy's law to the saturated porous disk of thickness Δz_d (L), saturated hydraulic conductivity K_d (L/T) and cross sectional area A (L^2), similarly as in Eching et al. (1994). One obtains the following expression of the drained outflow $Q(t)$ (L^3/T):

$$Q(t) = -K_d \frac{\Delta h_k(z=0,t) - \Delta h_i}{\Delta z_d} A = \frac{\Delta V(t)}{\Delta t} \tag{4}$$

where ΔV (L^3) is the extracted water volume during the time interval Δt. The following relation gives the changes in the increment of suction at the specimen bottom:

$$\Delta h_k(z=0,t) = \Delta h_i - \Delta z_d \frac{Q(t)}{AK_d} \tag{5}$$

This relation indicates that the change with respect to time of the suction applied at the specimen bottom can be derived from the monitoring of the drained outflow $Q(t)$, which depends on both K_d and the combined effects of the water retention and transfer properties of the unsaturated specimen. Theoretically, the case with no impedance effect in which $\Delta h_k(z=0,\ t) = \Delta h_i$ is met with porous disks of large K_d, when $K_d \gg Q(t)/A$.

Based on the time superposition principle (Hantush, 1964; Stanić et al., 2017, among others), it is hence proposed (i) to decompose a suction increment at the specimen bottom $\Delta h_k(z=0,\ t)$ as the sum of a number N_s of very small successive suction increments $\Delta h_m = \Delta h_i/N_s$, occurring at time t_m, (ii) to apply the analytical solution (equation (1)) to each suction increment, and (iii) to superpose in time all suction increments, giving the following expression of the suction changes:

$$\Delta h_k(z,t) = \sum_{m=1}^{N_s} \Delta h_m \left(1 - \frac{4}{\pi} \sum_{n=1,3,5...}^{\infty} \frac{1}{n} e^{-(n\pi/2)^2 (t-t_m) D(h_k)/H_s^2} sin\frac{n\pi z}{2H_s}\right) \tag{6}$$

resulting in the following expression of extracted volume:

$$V(t) = \frac{V_\infty}{N_s} \sum_{m=1}^{N_s} \left(1 - \frac{8}{\pi^2} \sum_{n=1,3,5...}^{\infty} \frac{1}{n^2} e^{-(n\pi/2)^2 (t-t_m) D(h_k)/H_s^2}\right) \tag{7}$$

Note that larger N_s secures smoother curves obtained using equations (6) and (7). Since the computation is not time-consuming, $N_s = 1{,}000$ is adopted for all cases. Also, for $N_s = 1$ equation (7) becomes similar to standard Gardner's solution (equation (2)).

As in Gardner's method, $K(h_k)$ is calculated as $D(h_k)C(h_k)$, where $C(h_k) = \Delta\theta/\Delta h_i$ is determined from the measured WRC ($\Delta\theta$ is the measured change of water content over the suction step Δh_i). $D(h_k)$ is adjusted to obtain the best agreement between equation (7) and the experimental points describing the water outflow, by optimizing the squared correlation coefficient R^2. In Figure 1, the changes in suction along the specimen's height at different times are presented. Without any impedance effects (dotted lines), equation (1) is used to calculate suction profiles (dotted lines), where the calculated $\Delta h_k(z{=}0,\ t)$ immediately reaches Δh_i. In the case of impedance effects, the suction profiles (solid lines) are calculated using equation (6). The calculated changes in suction with time at specimen bottom show how the boundary conditions progressively reach the Δh_i condition imposed at $t = 0$ at the bottom of the porous disk.

Given that the calculation of the Fourier series of equations (1), (2), (6), and (7) may be found somewhat tedious, one tested the approximated empirical formula proposed by Sivaram and Swamee (1977) in their simplified approach to solve Terzaghi-Fröhlich's consolidation equation. This expression, that exhibits a difference with analytical solution smaller than 1% for $0\% < V(t)/V_\infty < 90\%$ and less than 3% for $90\% < V(t)/V < 100\%$, writes as follows:

$$\frac{V(t)}{V_\infty} = \left(\frac{4tD(h_k)}{\pi H_s^2}\right)^{0.5}\left(1+\left(\frac{4tD(h_k)}{\pi H_s^2}\right)^{2.8}\right)^{-0.179} \tag{8}$$

Substituting in all equations where Fourier series appear, equation (7) becomes

$$V(t) = \frac{V_\infty}{\Delta h_i}\left[\sum_{m=0}^{N_s}\Delta h_m - \sum_{m=0}^{N_s}\Delta h_m\left(1-\left(\frac{4(t-t_m)D(h_k)}{\pi H_s^2}\right)^{0.5}\left(1+\left(\frac{4(t-t_m)D(h_k)}{\pi H_s^2}\right)^{2.8}\right)^{-0.179}\right)\right] \tag{9}$$

For sake of simplicity, it is proposed to adopt expression ((9)) instead of equation (7).

2.3. A New Method to Account for Nonconstant Imposed Suction Increment

As observed in Stanić et al. (2019), Gardner's method can be valid at lower water contents, if the hydraulic conductivity of the unsaturated soil becomes smaller than that of the ceramic disk, reducing impedance effects to 0. In Stanić et al.'s (2019) device, given that smaller water quantities are extracted from the specimen at higher suctions, it is necessary, for a better accuracy, to monitor the water exchanges through the changes in height of the inner thin tube used for imposing the suction increment $\Delta h_i = \Delta h_k(z{=}0,\ t{=}0)$, as seen in Figure 2. Given that a gradual decrease in suction $\Delta h_k(z = 0,t)$ occurs once the mobile device has been lowered to water extraction, the standard Gardner's solution is valid only for sufficiently small values of the ratio $\frac{\Delta h_i - \Delta h_k(z=0,\ t_\infty)}{\Delta h_i}$ (see Stanić et al., 2019). Otherwise, it is necessary to account for the change in $\Delta h_k(z = 0,\ t)$.

Since the increase in water level is caused by the outflow drained from the specimen, the water balance equation can be written in the following way:

$$-\frac{d\Delta h_k(z=0,t)}{\mathrm{d}t}a_{it} = Q(t) = \frac{\mathrm{d}V(t)}{\mathrm{d}t} \tag{10}$$

where a_{it} is the cross-section area (L^2) of the small inner tube in which outflow is collected. Since there is no impedance effect, $V(t)$ can be substituted with Gardner's solution (equation (2)), by substituting V_∞ by $H_sA\Delta h_k(z=0,\ t)C(h_k)$, thus replacing the constant Δh_i by the nonconstant $\Delta h_k(z{=}0,\ t)$. The outflow $Q(t)$ then becomes equal to

$$Q(t) = \frac{\mathrm{d}V(t)}{\mathrm{d}t} = \frac{\mathrm{d}\Delta h_k(z=0,t)}{\mathrm{d}t}\,H_sAC(h_k)F(t) + H_sA\Delta h_k(z=0,t)C(h_k)F'(t) \tag{11}$$

where $F(t) = 1 - \frac{8}{\pi^2}\sum_{n=1,3,5\ldots}^{\infty}\frac{1}{n^2}e^{-(n\pi/2)^2\ \mathrm{t}\ \mathrm{D}(h_k)/H_s^2}$ and $F'(t) = \frac{\mathrm{d}F}{\mathrm{d}t}$.

After introducing equation (11) into equation (10), the variables can be separated, leading to

$$-\int_{\Delta h_i}^{\Delta h_k(z=0,t)} \frac{\mathrm{d}\Delta h_k(z=0,t)}{\Delta h_k(z=0,t)} = \int_0^t \frac{F'(t)H_sC(h_k)A}{a_{it}+F(t)H_sC(h_k)A}\mathrm{d}t \tag{12}$$

By integrating both sides of equation (12), the following obtains

$$\ln\left(\frac{\Delta h_i}{\Delta h_k(z=0,t)}\right) = \ln\left(1+F(t)\frac{H_sC(h_k)A}{a_{it}}\right) \tag{13}$$

The expression of $\Delta h_k(z{=}0,\ t)$ is then derived as follows:

$$\Delta h_k(z=0,t) = \frac{\Delta h_i}{1+F(t)\frac{H_sC(h_k)A}{a_{it}}} \tag{14}$$

Since V_∞ is equal to the total volume of water collected in the tube between $t = 0$ and $t = t_\infty$, the following equation can be written as follows:

$$V_\infty = a_{it}(\Delta h_i - \Delta h_k(z=0,t_\infty)) = H_sA\Delta h_k(z=0,t_\infty)C(h_k) \tag{15}$$

$$\frac{H_sC(h_k)A}{a_{it}} = \frac{\Delta h_i}{\Delta h_k(z=0,t_\infty)} - 1 \tag{16}$$

After introducing the last expression into equation (14), the final forms of $\Delta h_k(z{=}0,\ t)$ and $V(t)$ are obtained:

$$\Delta h_k(z=0,t) = \frac{\Delta h_i}{1+F(t)\left(\frac{\Delta h_i}{\Delta h_k(z=0,t_\infty)}-1\right)} \tag{17}$$

$$V(t) = a_{it}\Delta h_i\left(1-\frac{1}{1+F(t)\left(\frac{\Delta h_i}{\Delta h_k(z=0,t_\infty)}-1\right)}\right) \tag{18}$$

For $t = 0$, $F(t) = 0$, so $\Delta h_k(z{=}0,\ t{=}0) = \Delta h_i$ and $V(t) = 0$. On the contrary, for $t = t_\infty$, $F(t) = 1$, leading to $\Delta h_k(z{=}0,\ t_\infty)$ and $V(t) = a_{it}(\Delta h_i - \Delta h_k(z{=}0,\ t_\infty)) = V_\infty$. Like in the standard Gardner's method, $K(h_k)$ is determined based on adjusting the value of $D(h_k)$ by comparing our solution (equation (18)) with experimental data. The value of $C(h_k) = \Delta\theta/\Delta h_k(z{=}0,\ t_\infty)$ is calculated based on the corresponding suction step on the measured $\Delta\theta$ taken from WRC. Unlike equation (9) or (7), equation (18) cannot be mathematically reduced to standard Gardner's solution (equation (2)), since for $\Delta h_k(z{=}0,\ t_\infty) = \Delta h_i$ there will be no outflow — $V(t) = 0$. Please note that Fourier series $F(t)$ is identical as in equation (2); thus, it can be substituted using the empirical expression (8), as previously explained, and introduced into equation (18) for sake of simplicity.

To calculate suction profiles, the nonconstant boundary condition (equation (17)) is decomposed as in the case of the impedance effect, and equation (6) is applied afterward. Figure 2 presents the calculated suction profiles at different times for two cases: (i) constant suction step $\Delta h_i = \Delta h_k(z{=}0,\ t_\infty)$ described using equation (1) — dotted line — and (ii) nonconstant suction increment $\Delta h_i = \Delta h_k(z{=}0,\ t)$ described with equation (6) — solid line.

3. Experimental Investigations

This work was initially developed when investigating the water retention and transfer properties of a volcanic coarse substrate used in an urban green roof in the Paris area, detailed in Stanić et al. (2019). The validity of the method is further established by also considering the experimental data obtained on two quite different materials (a poorly graded sand and an undisturbed silty clay) published by Wayllace and Lu (2011).

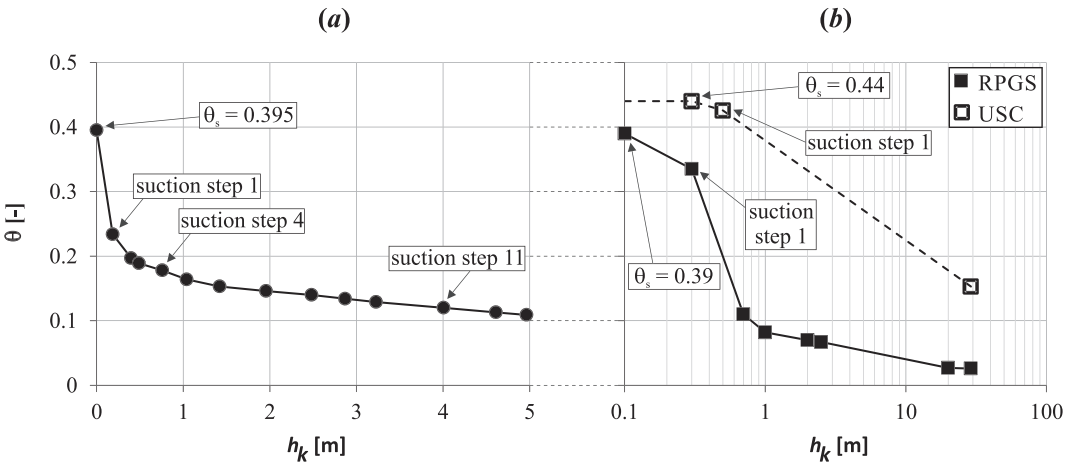

Figure 3. WRCs of (a) the coarse substrate determined by Stanić et al. (2019) and (b) of the remolded poorly graded sand (RPGS) and undisturbed silty clay (USC) determined by Wayllace and Lu (2011). Saturated water content (θ_s) is indicated in each graph.

3.1. Data of Stanić et al. (2019)

In the device of Stanić et al. (2019) (Figures 1 and 2), a 70-mm diameter and 24-mm height specimen is placed on a Δz_d = 5-mm-thick ceramic porous disk with an air entry value of 50 kPa, and a saturated hydraulic conductivity $K_d = 4.02 \times 10^{-8}$ m/s. Water exchanges are monitored by using an inner tube (inner diameter 5 mm, outer diameter 8 mm) and an outer tube (inner diamater 15 mm). The maximum height allowed by the system is equal to 5 m, corresponding to a maximum suction of 50 kPa. The material investigated was the volcanic substrate used for covering the "Green Wave" in the city of Champs-sur-Marne in France (Versini et al., 2018). The substrate is a coarse granular material with 4% of organic matter, an average grain density of 2.35 Mg/m^3 and a bulk density of 1.42 Mg/m^3 (porosity of 0.395), with D_{50} = 1.5 mm, 15% particles smaller than 80 μm and a curvature coefficient ($D_{30}{}^2/(D_{10}\,D_{60})$) of 1.95. The saturated hydraulic conductivity of the substrate is $K_s = 8.11 \times 10^{-6}$ m/s, and its WRC is given in Figure 3a (Stanić et al., 2019).

3.2. Data of Wayllace and Lu (2011)

Wayllace and Lu (2011) developed a transient water release and imbibition method for determining the WRC and HCF of two materials along the drying and wetting paths, by imposing, through the axis translation method, two suction increments for draining water from the soil specimen, followed by a suction decrease allowing subsequent water imbibition. The transient water release and imbibition apparatus consisted of (i) a flow cell accommodating a soil specimen of 60.7-mm diameter placed on 300-kPa high air entry value ceramic disk (saturated hydraulic conductivity $K_d = 2.5 \times 10^{-9}$ m/s, thickness Δz_d = 3.2 mm), (ii) a pressure regulator connected to cell top, and (iii) a water jar placed on a weight scale connected to cell bottom to collect the drained outflow (more details in Wayllace & Lu, 2011). During drainage, a first imposed suction increment was fixed (2 kPa), just above the specimen air entry values, small enough to just initiate the outflow from the specimen, while the second step was significantly larger (about 300 kPa).

Wayllace and Lu investigated two different soils: a remolded poorly graded sand compacted to a porosity of 0.39 and an undisturbed silty clay with a porosity 0.44. The values of the saturated hydraulic conductivities of these soils are $K_s = 2.1 \times 10^{-6}$ m/s and 1.1×10^{-7} m/s, respectively, and their WRCs are presented in Figure 3b. The significantly lower saturated hydraulic conductivity of the ceramic disk clearly indicates that impedance effects have to be accounted for when analyzing the outflow data.

4. Determination of Hydraulic Conductivity Values

4.1. Coarse Volcanic Substrate of the Green Wave

By analyzing the evolution of drained outflow for different suction steps, the change in hydraulic conductivity with respect to increased suction is obtained (Stanić et al., 2019). Thirteen suction steps were carried out, where Steps 1 and 2 were constant suction steps (with the overflow system of Figure 1), whereas the remaining steps correspond to nonconstant suction increments (see Figure 2). The saturated hydraulic

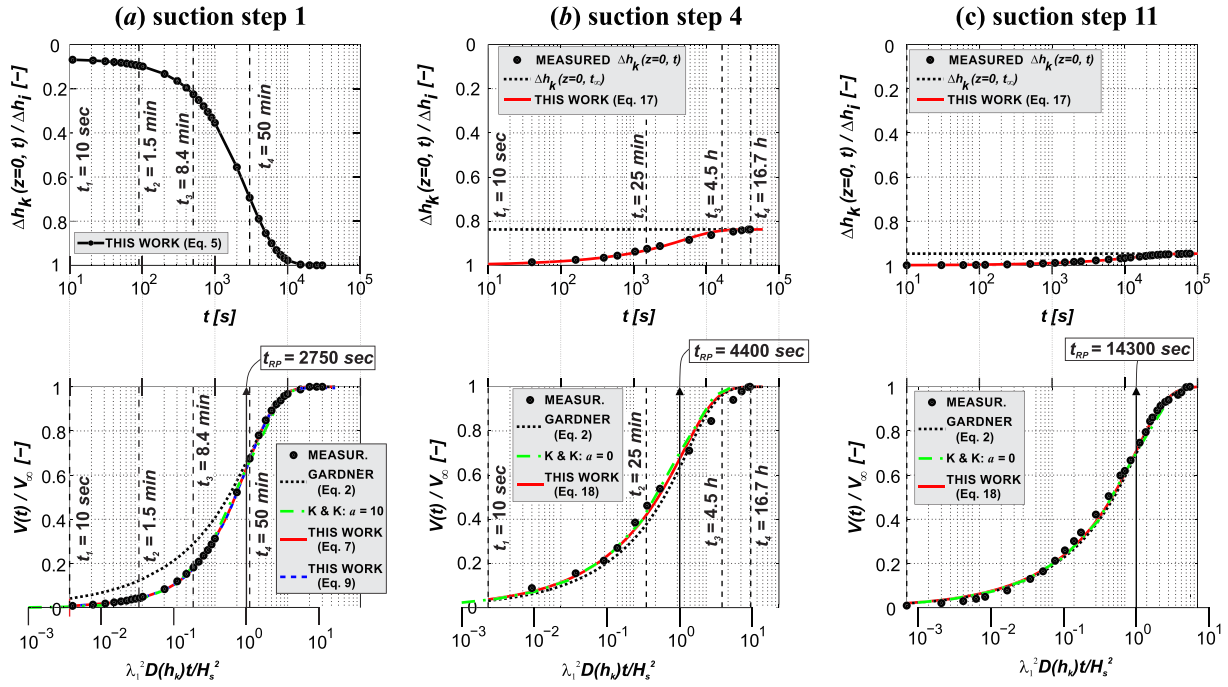

Figure 4. Green Wave substrate; top graphs — suction change at specimen bottom, at contact with ceramic disk; bottom graphs — measured outflow (circles) compared with calculated values from different methods (indicated on the figure); (a) Suction Step 1 — impedance effect; (b) Suction Step 4 — nonconstant suction increment; (c) Suction Step 11 — same as in (b).

conductivities of both the specimen (K_s) and the ceramic disk (K_d) were determined using a constant head hydraulic conductivity test described in details in Stanić et al. (2019).

In the top graph of Figure 4*a* is illustrated the evolution of $\Delta h_k(z{=}0, t)$ for Step 1 (connected filled dots), calculated using measured volumes and Darcy's law (equation (5)), that gradually reaches Δh_i imposed at the disk bottom. It can be noticed that the ratios $\Delta h_k(z{=}0, t)/\Delta h_i$ at different times (t_1 to t_4) correspond to those in Figure 1 (x axis) for the same t.

The bottom graph of Figure 4a presents a comparison of the calculated values of $V(t)/V_\infty$ (in a time logarithmic scale) using Gardner's method, Kunze and Kirkham's method and that developed in this work. The best fit between equation (9) and experimental data is obtained for $D(h_k = 18.5\text{ cm}) = 1.2 \times 10^{-6}$ m^2/s, where $C(h_k = 18.5\text{ cm}) = 0.16/0.185 = 0.86$ m^{-1} (see Figure 3a), which finally gives $K(h_k = 18.5\text{ cm}) = 1.04 \times 10^{-6}$ m/s. Fitting our experimental data following Kunze and Kirkham's method (nondimensional time variable $\lambda_1^2 D(h_k) t_{RP}/H_s^2$ is also reported on the bottom x axis, see Appendix B) provided $\lambda_1 = 0.097$ and $t_{RP} \approx$ 2,750 s, with $a = 10$. The case of Suction Step 1 is described in detail in Appendix B to point out the difficulties typical of graphical methods. Finally, the best overall agreement with measurements is obtained for $a =$ 10 (having on mind that $a = 1{,}000$ provides a hydraulic conductivity higher than the saturated one). The figure shows excellent agreement between experimental data and both Kunze and Kirkham and the proposed method. Unsurprisingly, the extracted volume estimated by Gardner's method ($D(h_k) = 7.5 \times 10^{-8}$ m^2/s) for times smaller than 1 h is higher than the measured one and that calculated with the two other methods.

In case of Step 4 (initial suction 0.489 m and $\Delta h_i = 0.321$ m with 17% of suction step change), calculated changes in $\Delta h_k(z{=}0, t)$ (equation (17) — solid line) are compared with the measured changes in water level in the top graph of Figure 4b, whereas calculated (equation (18)) and measured drained volumes are compared in the bottom graph. In this case $C(h_k) = \Delta\theta/\Delta h_k(z{=}0, t_\infty) = 0.04$ m^{-1}, where $\Delta\theta = 0.011$ and $\Delta h_k(z{=}0, t_\infty) = (1{-}0.17)\ x\ \Delta h_i = 0.266$ m (see Figure 3a). The difference between the nonconstant ($\Delta h_k(z{=}0, t)$) and constant ($\Delta h_k(z{=}0, t_\infty)$) suction increment is more significant at initial time, right after imposing Δh_i, while the largest difference in drained volumes between our method and Gardner's method is observed after $t_2 = 25$ min. The method proposed in this work shows the best agreement for $D(h_k) = 4.3 \times 10^{-8}$ m^2/s (the same value is adopted for Gardner's method), while Kunze and

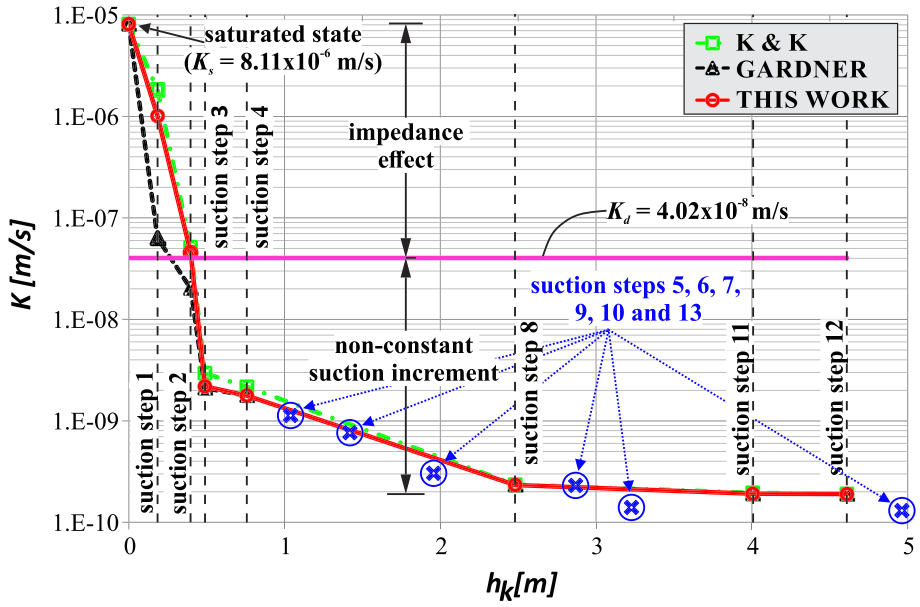

Figure 5. Change of hydraulic conductivity of the coarse substrate with respect to increased suction obtained using three different methods: Kunze and Kirkham's method (squares), Gardner's method (triangles), and methods developed in this work (circles). Hydraulic conductivity values obtained by analyzing volume change measurements at larger times (equation (3)) are presented with blue symbols.

Kirkham's theoretical curve with parameters $a = 0$, $t_{RP} \approx 4{,}400$ s and $\lambda_1^2 = 2.467$ also shows satisfying agreement at small times. All three methods show almost identical agreement with measured volumes when the overall suction step change is negligible, like in Step 11 (initial suction 3.227 m and $\Delta h_i = 0.822$ m with 5% of suction step change) presented in Figure 4c (Gardner's and our method — $D(h_k) = 1.6 \times 10^{-8}$, Kunze and Kirkham's method — $a = 0$, $t_{RP} \approx 14{,}300$ s and $\lambda_1^2 = 2.467$). Concerning the methods proposed in this work, $R^2 > 0.99$ for all three steps presented.

The accuracy of the determined $K(h_k)$ value depends on the accuracies of both the WRC measurements (parameter $C(h_k)$) and the outflow measurements (fitted value of $D(h_k)$), both governed by the precision of the differential pressure transducer (±0.05 mm). The relative uncertainty of $K(h_k)$ can be expressed as follows:

$$\frac{\delta K(h_k)}{K(h_k)} = \sqrt{\left(\frac{\delta D(h_k)}{D(h_k)}\right)^2 + \left(\frac{\delta C(h_k)}{C(h_k)}\right)^2} \tag{19}$$

The uncertainty of $C(h_k) = \Delta\theta/\Delta h_i = V_\infty/(H_s A \Delta h_i)$ depends on the uncertainties of V_∞, H_s, and Δh_i, and it can be expressed as follows:

$$\frac{\delta C(h_k)}{C(h_k)} = \sqrt{\left(\frac{\delta V_\infty}{V_\infty}\right)^2 + \left(\frac{\delta H_s}{H_s}\right)^2 + \left(\frac{\delta \Delta h_i}{\Delta h_i}\right)^2} \tag{20}$$

where $\delta V_\infty = \pm 6.32 \times 10^{-9}$ m^3 ($\pm 9.82 \times 10^{-10}$ m^3) when measuring in the outer (inner) tube, $\delta H_s = \pm 0.1$ mm and $\delta \Delta h_i = \pm 0.5$ mm. In case of all three suction steps presented, $\frac{\delta C(h_k)}{C(h_k)} \approx 0.5\%$. Furthermore, it appears that the uncertainties of the outflow measurements (few percent at small times, and less than 1% for $t > 5$ min) have no significant impact on $D(h_k)$ value, adjusted based on the R^2 criterion $\left(\frac{\delta D(h_k)}{D(h_k)} \approx \frac{\delta C(h_k)}{C(h_k)} \approx 0.5\%\right)$. Finally, the relative uncertainty of hydraulic conductivity can be calculated based on equation (19) as $\frac{\delta K(h_k)}{K(h_k)} \approx \sqrt{2\left(\frac{\delta C(h_k)}{C(h_k)}\right)^2} \approx \sqrt{2} \times 0.5\% \approx 0.71\%$. Given that the hydraulic conductivity changes over 5 orders of magnitude in the case of the coarse volcanic material (see Figure 5), this value is satisfactory.

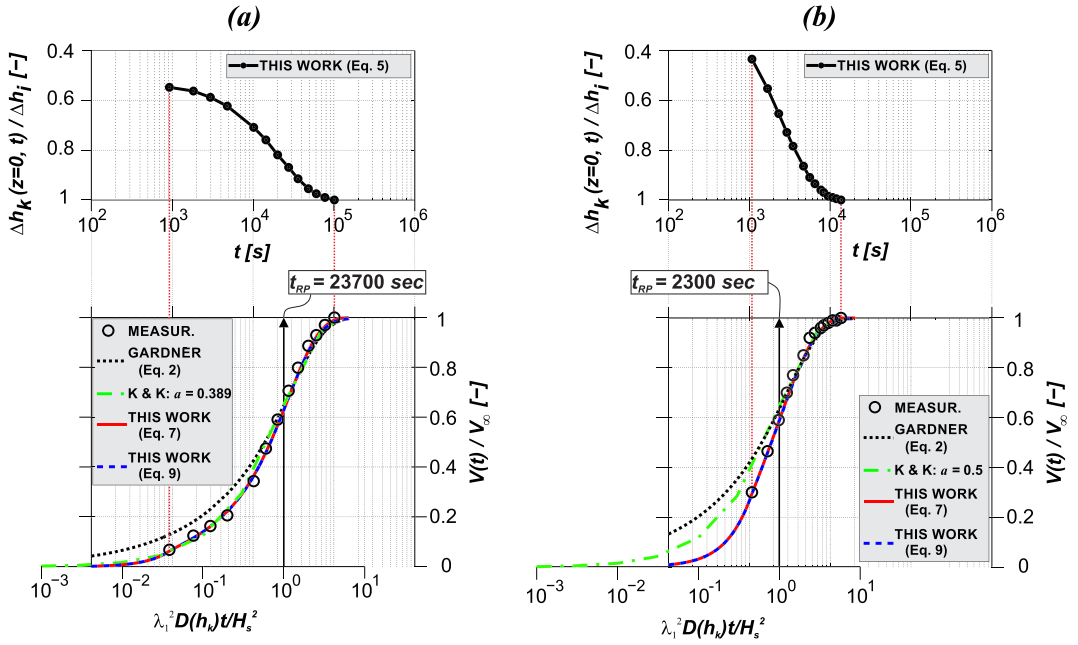

Figure 6. (a) Poorly graded sand (data from Wayllace & Lu, 2011): (top) Suction change at specimen bottom, at contact with ceramic disk; (bottom) Measured outflow (circles) compared with calculated values from different methods (indicated on the figure). (b) Undisturbed silty clay (data from Wayllace & Lu, 2011): same as in (a)

Figure 5 shows the changes in hydraulic conductivity obtained by using the three different approaches: Gardner's method (triangles), Kunze and Kirkham's method (squares) and the methods proposed in this work (circles). All three methods are applied on Steps 1, 2, 3, 4, 8, 11, and 12, for which stable and reliable volume change measurements are obtained at small times. Note that we also present in the Figure the hydraulic conductivity values for Steps 5, 6, 7, 9, 10, and 13, which were obtained by using the standard Gardner's method, based on volume change measurements at larger times (equation (3)).

Figure 5 shows that both our method and Kunze and Kirkham's one provide very similar results for the first two steps, where significant impedance effect occurs. In this range, Gardner's method unsurprisingly provides significantly lower $K(h_k)$ values because it integrates the effect of the low hydraulic conductivity of the disk. However, the difference between the three methods decreases quite rapidly, with convergence observed at $K(h_k) = 2 \times 10^{-8}$ m/s, to compare to the twice larger K_d value of the ceramic disk (4.02×10^{-8} m/s). In case of Steps 8, 11, and 12, where the imposed suction step changes less than 5 % with no impedance effect, all methods provide comparable results.

From a hydrological point of view, the values of $K(h_k)$ in the low suction regime are of the greatest interest, since they have the most significant influence on the hydrological responses of the soil (substrate). As shown in Figure 5, this zone (first four steps) is precisely that in which the most significant differences are observed between the methods used, showing the advantage of our method, that is less operator-dependent compare to that of Kunze and Kirkham.

4.2. Poorly Graded Sand and Silty Clay

Among the transient outflow data from Wayllace and Lu (2011), only the first and smallest of the two applied suction steps was considered on both specimens because (i) our method assumes constant diffusivity, a hypothesis only acceptable for small suction increments and (ii) the impedance effect is more significant at initial steps, when the hydraulic conductivity of the soil is significantly larger than that of the ceramic disk.

In Figure 6 are presented the same kind of data as in Figure 4 for the poorly graded sand (Figure 6a) and the silty clay specimens (Figure 6b). In the first case $H_s = 2.67$ cm, $\Delta h_i = 0.2$ m and $V_\infty = 4.66 \times 10^{-6}$ m^3, while in

Table 1
Parameters Used and Hydraulic Conductivity Values Obtained for Gardner's Method, Our Method and Kunze and Kirkham's Method for the Poorly Graded Sand and the Undisturbed Silty Clay Investigated in Wayllace and Lu (2011)

	Gardner		This work		Kunze and Kirkham			
	D (m^2/s)	K (m/s)	D (m^2/s)	K (m/s)	a (−)	t_{RP} (s)	$\lambda_1{}^2$ (−)	K (m/s)
Poorly graded sand	1.0×10^{-8}	3.01×10^{-9}	1.8×10^{-8}	5.43×10^{-9}	0.389	23700	1.3228	6.87×10^{-9}
Undisturbed silty clay	8×10^{-8}	5.73×10^{-9}	5.0×10^{-7}	3.58×10^{-8}	0.5	2300	1.1596	1.59×10^{-8}

the case of silty clay $H_s = 2.41$ cm, $\Delta h_i = 0.2$ m, and $V_\infty = 1 \times 10^{-6}$ m^3. The bottom graphs in Figure 6a show that our method and Kunze and Kirkham's method compare quite well, whereas Gardner's method overestimates the outflow values at small times, like for the Green Wave substrate (Figure 4a). On the contrary, for the silt clay specimen (Figure 6b, bottom) both Gardner's and Kunze and Kirkham's methods overestimate the outflows at small times, whereas our method shows excellent agreement with measurements along the whole time range. Due to the poor agreement at small times, Kunze and Kirkham's analytical curve was fitted with measurements at larger times (the parameters for this method are presented in Table 1).

Based on the adjusted $D(h_k)$ values in the case of Gardner's and our method, and on parameters a, t_{RP} and $\lambda_1{}^2$ in case of Kunze and Kirkham's method, the values of the hydraulic conductivity for the first step were determined (see Table 1). Based on the data from both our method and Kunze and Kirkham's one, it can be concluded that the impedance effect occurs for both soils ($K(h_k) > K_d$), especially in case of silty clay where calculated $K(h_k)$ values are about an order of magnitude larger than K_d for both methods. As in case of the coarse substrate, Gardner's method provides significantly lower $K(h_k)$ values compared to those determined using our and Kunze and Kirkham's method.

4.3. On the Occurrence of Impedance Effects

The most convenient way to clarify the importance of impedance effects is by analyzing the evolution of the ratio $\Delta h_k(z=0, t)/\Delta h_i$, calculated by using equation (5). The faster the ratio gets close to 1, the less significant impedance effects are, and vice versa. It seems reasonable in this regard to define a criterion based on the relative time t/t_∞ (t_∞ is the time at which equilibrium is reached) at which $\Delta h_k(z=0, t)/\Delta h_i$ gets close enough to 1 (ex. 0.95). Based on experience, we believe that impedance can be ignored if $\Delta h_k(z=0, t)/\Delta h_i$ reaches 0.95 within the first 5% of the step duration, leading to a criterion $t_c/t_\infty = 0.05$. After dividing both sides of equation (5) by Δh_i and introducing the proposed criterion, the following is obtained:

$$\frac{V(t_c)}{t_c A} < 0.05 \frac{\Delta h_i}{\Delta z_d} K_d, \qquad t_c = 0.05 t_\infty \tag{21}$$

Equation (21) shows that, besides the hydraulic conductivity K_d of the ceramic disk, the values of imposed suction increment Δh_i and stone thickness Δz_d also affect the impedance. For the data presented in Figure 4a (coarse material), Figure 6a (sand), and Figure 6b (silty clay), the values of the left side of equation (21) are 1.2×10^{-6}, 6.8×10^{-8}, and 9.6×10^{-8} m/s, respectively, while the values on the right side are 1.5×10^{-7}, 7.81×10^{-9}, and 7.81×10^{-9} m/s. Equation (21) is hence not satisfied in none of the three cases, meaning that impedance effects cannot be neglected. In case of Step 2 of the coarse substrate, the left and right sides of equation (21) are almost identical, which is in agreement with the obtained $K(h_k)$ value that is rather close to K_d (see Figure 5).

5. Conclusion

This paper presented two improvements to Gardner's method that were carried out (i) to account for impedance effect in a simpler and more objective way than in Kunze and Kirkham's graphical method and (ii) to

account for conditions in which nonconstant suction increment is applied, as is often the case in hanging column techniques.

The experimental data from various materials analyzed (coarse substrate, poorly graded sand, and undisturbed silty clay) in this work showed that the proposed simple analytical method fairly well accounts for the impedance effects of the ceramic disk. This method is believed to be more reliable than Kunze and Kirkham's graphical method, especially in the case of significant impedance effect, because it is not dependent of the difficulty in choosing the best fitting theoretical curve, among the family of curves provided by Kunze and Kirkham. The proposed method, based on the analytical resolution of the water transfer equations in the different parts of the system, only requires the accurate monitoring of outflow measurements, a requirement that is typical for any method for determining the hydraulic conductivity of multiphase porous material. The boundary condition in which a nonconstant suction increment is applied, which is often the case when using the hanging column technique, was also treated analytically to be applied in the (larger) suction area in which no impedance effect has to be considered, with also good agreement between measured and calculated values. It has also been shown, that the simplified equation of Sivaram and Swamee (1977) could successfully replace the analytical solution in Fourier series, which simplifies the use and improves the efficiency of the method. Compared to numerical back analyses method, this method provides point values of hydraulic conductivity without the need to assume a parametric expression for the conductivity function. Thus, it is not confronted with the issue of model selection. Also, this method is considered simpler in the sense that it does not require the use of any numerical simulations with optimization algorithms, since the analysis of outflow data and the derivation of hydraulic conductivity value is much more straightforward.

Appendix A: Gardner's Method

Gardner's method is based on both Richards equation (A1) and the Terzaghi-Fröhlich consolidation equation (equation (1)). In 1-D condition with vertical water flux, as in the case of Stanić et al.'s (2019) experimental device, Richards equation writes as follows:

$$\frac{\partial\theta(z,t)}{\partial t} = -\frac{\partial}{\partial z}\left(K(h_k)\left(\frac{\partial h_k(z,t)}{\partial z}+1\right)\right) \tag{A1}$$

where z is defined by a vertical axis oriented upward ($z = H$ — top surface; $z = 0$ — bottom surface), t is time (T), θ is the volumetric water content (−), and $K(h_k)$ the hydraulic conductivity (L/T). The effects of gravity are accounted by the term +1 in the right side, which accounts for the changes in hydraulic conductivity with respect to z.

Integration of Richards equation according to z, and multiplication with specimen cross-sectional area A (L^2) gives a simple water balance equation: $dV(t)/dt = Q(t)$, where $Q(t)$ is expressed as the multiplicative of A and the flux at the specimen bottom ($z = 0$):

$$Q(t) = -AK(h_k)\left(\left.\frac{\partial h_k(z,t)}{\partial z}\right|_{z=0}+1\right) \tag{A2}$$

Since the change in volume $V(t)$ is measured during the suction step outflow test, equation (A2) should be integrated with respect to time (from 0 to t):

$$V(t) = -A\int_0^t K(h_k)\left(\left.\frac{\partial h_k(z,t)}{\partial z}\right|_{z=0}+1\right)\mathrm{d}t \tag{A3}$$

Based on the representation of $h_k(z, t)$ elaborated in the main text, the gradient $\left.\frac{\partial h_k(z,t)}{\partial z}\right|_{z=0}$ can be presented as follows:

$$\left.\frac{\partial h_k(z,t)}{\partial z}\right|_{z=0} = \frac{\partial h_k(z,t=0)}{\partial z} + \left.\frac{\partial \Delta h_k(z,t)}{\partial z}\right|_{z=0} = -1 + \left.\frac{\partial \Delta h_k(z,t)}{\partial z}\right|_{z=0} \quad \text{(A4)}$$

where $\frac{\partial h_k(z,t=0)}{\partial z} = -1$ corresponds to hydrostatic conditions (equilibrium state) established at $t = 0$. By using equation (1) to describe $\Delta h_k(z,t)$, the derivative presented in equation (A4) at $z = 0$ can be expressed as follows:

$$\left.\frac{\partial h_k(z,t)}{\partial z}\right|_{z=0} = -1 - \frac{2\Delta h_i}{H_s} \sum_{n=1,3,5\ldots}^{\infty} e^{-(n/2)^2\pi^2 \frac{tD(h_k)}{{H_s}^2}} \quad \text{(A5)}$$

As explained in the text, Gardner's method assumes $D(h_k)$ = const. and $C(h_k)$ = const. along the imposed suction step (Δh_i), leading to $K(h_k) = D(h_k)C(h_k)$ = const. over the same Δh_i. Based on this and by using equation (A6) to describe the suction gradient at specimen bottom, equation (A3) can be presented in the following form:

$$V(t) = D(h_k)C(h_k)A\frac{2\Delta h_i}{H_s}\sum_{n=1,3,5\ldots}^{\infty}\int_0^t e^{-(n/2)^2\pi^2\frac{tD(h_k)}{{H_s}^2}}\mathrm{d}t \quad \text{(A6)}$$

giving, after solving the time integral in equation (A6):

$$V(t) = -H_s\Delta h_i C(h_k)A\frac{8}{\pi^2}\sum_{n=1,3,5\ldots}^{\infty}\frac{1}{n^2}\left(e^{-(n/2)^2\pi^2\frac{tD(h_k)}{{H_s}^2}} - 1\right) \quad \text{(A7)}$$

Since the total water volume drained is $V_\infty = H_s\Delta h_i C(h_k)A = H_s\Delta\theta A$ and $\frac{8}{\pi^2}\sum_{n=1,3,5\ldots}^{\infty}\frac{1}{n^2} = 1$, equation (A7) can be transformed into the final form of Gardner's method described with equation (2) in the main text.

Appendix B: Kunze & Kirkham's Method

Kunze and Kirkham's solution is graphically presented through various curves showing the changes in $V(t)/V_\infty$ with respect to the variable ${\lambda_1}^2 D(h_k)t/{H_s}^2$, in which parameter λ_1 is the first solution of the equation $a\lambda_n = cot(\lambda_n)$ (a is the ratio between the impedance of the ceramic disk and that of the specimen). The various curves correspond to various values of parameter a (see Figure 7). By shifting theoretical curves along the time axis (top x axis in Figure 7), the curve that shows the best agreement with experimental data (presented in the form $V(t)/V_\infty$ versus t) is chosen to define the value of a. A reference time t_{RP} is also graphically determined for ${\lambda_1}^2 Dt/{H_{soil}}^2 = 1$ (arrow in Figure 7). Kunze and Kirkham (1962) remarked that only a portion of the experimental data corresponded to the theoretical curves, so they recommended to rather fit the curves at small times. Based on the chosen value of a, the corresponding value of ${\lambda_1}^2$ is adopted from the table presented in Kunze and Kirkham (1962), and used to calculate diffusion coefficient as $D(h_k) = {H_s}^2/{\lambda_1}^2 t_{RP}$ and the hydraulic conductivity as $K(h_k) = D(h_k)\Delta\theta/\Delta h_i$.

In Figure 7 is presented an example that illustrates some level of subjectivity of this graphical method. If one follows the recommendation to fit only a portion of measurements (circles) at small times with theoretical curves (Figure 7a), curve $a = 0.2$ (solid line) seems to best match, as seen in log-log scale (left graph of Figure 7a). On the contrary, a time logarithmic scale (Figure 7a, right) gives better insight on the overall agreement, showing a significant deviation between the curve $a = 0.2$ and measurements for $t > 1{,}000$ s. By shifting the family of curves to the left (reducing t_{rp}), the best agreement over the entire range of t is obtained for $a = 10$ (solid line in Figure 7b, right), which is however not observable in log-log scale (left graph in Figure 7b). In addition, the deviation between different theoretical curves becomes less observable for higher a values (stronger impedance), which makes choosing the adequate curve even more difficult (e.g., $a = 10$ and $a = 1{,}000$ are almost overlapping — Figure 7b).

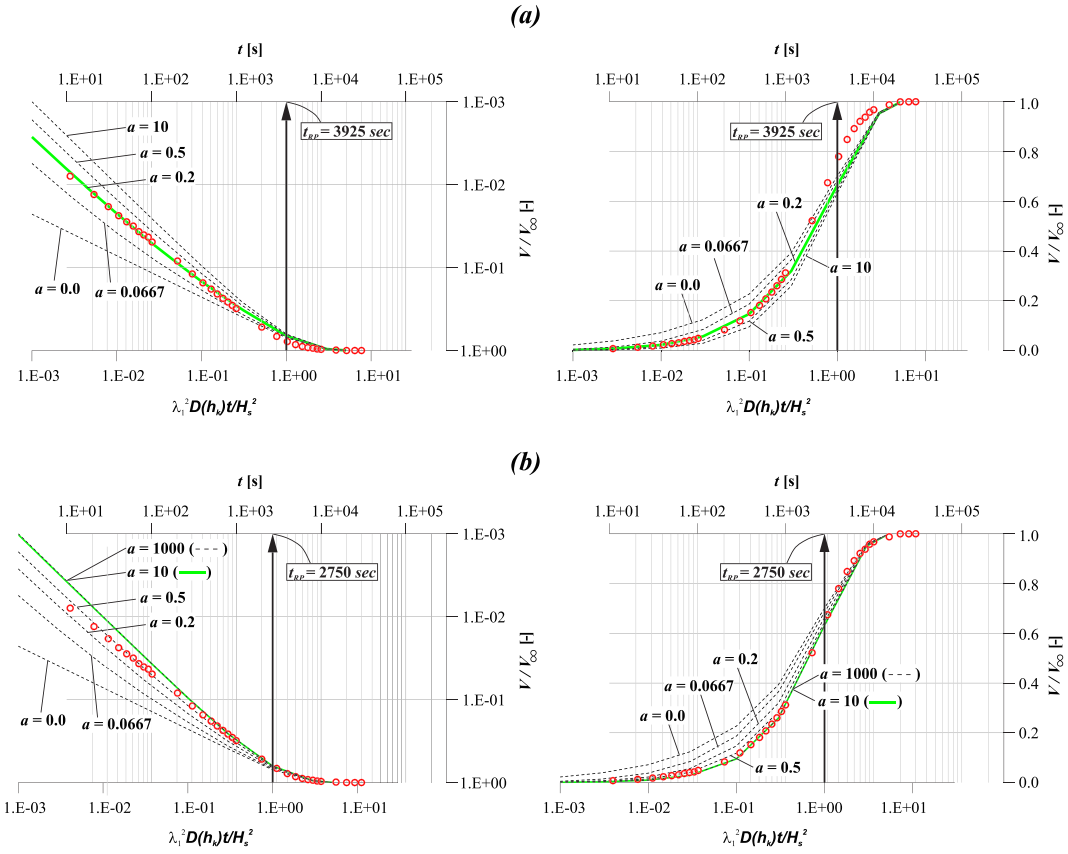

Figure 7. Correspondence between measured data (circles) and theoretical curves presented in log-log scale (left graphs) and time logarithmic scale (right graphs); (a) theoretical curves (and axis $\lambda_1^2 D(h_k)t/H_s^2$) are shifted from t_{rp} = 1E+4 s (initial position) to t_{rp} = 3,925 s to obtain the best agreement with data at small times (a = 0.2, solid line); (b) best overall fit between data and curves is obtained for t_{rp} = 2,750 (a = 10, solid line).

Acknowledgments
The authors greatly acknowledge the Inter-laboratory PhD Merit Scholarship, provided by Ecole des Ponts ParisTech to the first author, which made this collaborative work possible. A partial financial support by the Chair "Hydrology for resilient city" endowed by Veolia is also highly acknowledged. Data are archived in Zenodo repository.

References

Brooks, R. H., & Corey, A. T. (1964). Hydraulic properties of porous media. Hydrology papers, no. 3, Colorado State University, Fort Collins.
Doering, E. J. (1965). Soil-water diffusivity by the one-step method. *Soil Science*, *99*, 322–326.
Durner, W., & Iden, S. C. (2011). Extended multistep outflow method for the accurate determination of soil hydraulic properties near water saturation. *Water Resources Research*, *47*, W08526. https://doi.org/10.1029/2011WR010632
Eching, S. O., & Hopmans, J. W. (1993). Optimization of hydraulic functions from transient outflow and soil water pressure data. *Soil Science Society of America Journal*, *57*, 1167–1175.
Eching, S. O., Hopmans, J. W., & Wendroth, O. (1994). Unsaturated hydraulic conductivity from transient multistep outflow and soil water pressure data. *Soil Science Society of America Journal*, *58*, 687–695.
Fredlund, D. G., & Xing, A. (1994). Equations for the soil characteristic curve. *Canadian Geotechnical Journal*, *31*, 521–532.
Gardner, W. R. (1956). Calculation of capillary conductivity from pressure plate outflow data. *Soil Science Society Proceeding*, *20*(3), 317–320. https://doi.org/10.2136/sssaj1956.03615995002000030006x
Hantush, M. S. (1964). Hydraulics of Wells. In *Advances in Hydroscience* (ISSN: 0065-2768, (Vol. 1, pp. 281–432). Socorro, New Mexico: New Mexico Institute of Mining and Technology.
Khaleel, R., & Relyea, J. F. (1995). Evaluation of van Genuchten-Mualem relationships to estimate unsaturated hydraulic conductivity at low water contents. *Water Resources Research*, *31*(11), 2659–2668.
Kunze, R. J., & Kirkham, D. (1962). Simplified accounting for membrane impedance in capillary conductivity determinations. *Soil Science Society of America Proceedings*, *26*, 421–426. https://doi.org/10.2136/sssaj1962.03615995002600050006x
Levenberg, K. (1944). A method for the solution of certain non-linear problems in least squares. *Applications of Mathematics*, *2*, 164–168.
Miller, E., & Elrick, D. (1958). Dynamic determination of capillary conductivity extended for non-negligible membrane impedance. *Soil Science Society of America Proceedings*, *22*, 483–486.
Mualem, Y. (1976). A new model for predicting the hydraulic conductivity of unsaturated porous media. *Water Resources Research*, *12*(3), 513–522. https://doi.org/10.1029/WR012i003p00513
Nasta, P., Huynh, S., & Hopmans, J. W. (2011). Simplified multistep outflow method to estimate unsaturated hydraulic function for coarse texted soils. *Soil Science Society of America Journal*, *75*, 418–425.
Richards, L. A. (1931). Capillary conduction of liquids through porous media. *Physics*, *1*, 318–333.
Rijtema, P. E. (1959). Calculation of capillary conductivity from pressure plate outflow data with non-negligible membrane impedance. *Netherlands Journal of Agricultural Science*, *7*(3), 209–215.

Schelle, H., Iden, S. C., & Durner, W. (2011). Combined transient method for determining soil hydraulic properties in a wide pressure head range. *Soil Science Society of America Journal*, *75*, 1681–1693.

Šimunek, J., van Genuchten, M. T., & Šejna, M. (2008). Development and applications of the HYDRUS and STANMOD software packages and related codes. *Vadose Zone Journal*, *7*, 587–600. https://doi.org/10.2136/vzj2007.0077

Sivaram, B., & Swamee, P. (1977). A computational method for consolidation coefficient. *Soils Found. Tokyo*, *17*(2), 48–52.

Stanić, F., Cui, Y.-J., Delage, P., De Laure, E., Versini, P.-A., Schertzer, D., & Tchiguirinskaia, I. (2019). A device for the simultaneous determination of the water retention properties and the hydraulic conductivity function of an unsaturated coarse material; Application to a green-roof volcanic substrate. *Geotechnical Testing Journal*, *43*(3). https://doi.org/10.1520/GTJ20170443

Stanić, F., Jaćimović, N., Ranđelović, A., & Despotović, J. (2017). Laboratory investigation of hydraulic characteristics of fly ash as a fill material from the aspects of pollutant transport. *Water Science and Technology*, *76*(4), 976–982.

Terzaghi, K., & Fröhlich, O. K. (1936). *Theorie der Setzung von Tonschichten*. Leipzig: Wien, Franz Deuticke.

Valiantzas, J. D. (1990). Analysis of outflow experiments subject to significant plate impedance. *Water Resources Research*, *26*(12), 2921–2929.

van Dam, J. C., Stricker, J. N. M., & Droogers, P. (1994). Inverse method to determine soil hydraulic functions from multistep outflow experiments. *Soil Science Society of America Journal*, *58*, 647–652.

van Genuchten, M. T. (1980). A closed-form equation for predicting the hydraulic conductivity of unsaturated soils. *Soil Science Society of America Journal*, *44*(5), 892–898. https://doi.org/10.2136/sssaj1980.03615995004400050002x

Versini, P. A., Gires, A., Fitton, G., Tchiguirinskaia, I., & Schertzer, D. (2018). Toward an assessment of the hydrological components variability in green infrastructures: Pilot site of the Green Wave (Champs-sur-Marne). *La Houille Blanche*, *4*, 34–42.

Wayllace, A., & Lu, N. (2011). A transient water release and imbibitions method for rapidly measuring wetting and drying soil water retention and hydraulic conductivity functions. *Geotechnical Testing Journal*, *35*(1), 1–15.